

# LASER GUIDE STAR ADAPTIVE OPTICS ON THE 5.1 METER TELESCOPE AT PALOMAR OBSERVATORY

**Richard Dekany**

*Caltech Optical Observatories  
California Institute of Technology, Pasadena, CA 91125*

**Viswa Velur, Hal Petrie, Antonin Bouchez, Matthew Britton, Alan Morrissett, Robert Thicksten**

*Caltech Optical Observatories  
California Institute of Technology, Pasadena, CA 91125*

**Mitchell Troy, Chris Shelton, Tuan Troung, Jennifer Roberts, Gary Brack, Thang Trinh,  
Siddarayappa Bikkannavar, Steve Guiwitz, John Angione, Fang Shi**

*Jet Propulsion Laboratory  
California Institute of Technology, Pasadena, CA 91109*

**Edward Kibblewhite**

*The Enrico Fermi Institute  
University of Chicago, Chicago, IL 60637*

## ABSTRACT

The 5.1 meter diameter telescope at Palomar Observatory has been equipped with a (currently) 7.5 W sodium D<sub>2</sub>-line micropulse/macropulse solid-state sum-frequency Nd:YAG slab laser for use with the existing 241-actuator Palomar Adaptive Optics System (PALAO). The combination of the pulsed laser, developed at University of Chicago, and the natural guide star AO system, which alone can achieve 80% K-band Strehl ratio (175 nm rms residual wavefront error) running at 2 kHz sample rates, will allow near-term atmospheric compensation to resolutions as fine as 50 milliarcseconds (240 nanoradians) over a significant fraction of the sky.

As final testing of the laser guide star (LGS) system is completed, we are simultaneously planning for a major PALAO system upgrade to utilize a new 3,217 active-actuator deformable mirror. If fully funded, PALM-3000 will suppress wavefront error to as low as 80 nm rms using bright natural guide stars in excellent seeing conditions, providing ~20% Strehl ratio at 0.4  $\mu\text{m}$  wavelength resulting in 16 milliarcsec (78 nanoradian) resolution. PALM-3000 will enable visible science observations of solar system bodies and enable unprecedented infrared studies of companions in orbit around nearby stars. Low-risk upgrades of the current pulsed sodium laser should achieve 15-20W average power for use with the upgraded PALM-3000 system.

## 1. PALM-LGS SYSTEM DESCRIPTION

The Palomar Adaptive Optics System (PALAO) has been operating successfully on the 5.1 meter (200-inch) diameter Hale Telescope at Palomar Mountain since 1999. Originally optimized for science operation between 1.25 and 2.4 microns imaging wavelength, PALAO has been the 2<sup>nd</sup> most highly subscribed instrument at Palomar, introducing a generation of astronomers to adaptive optics technology. Since October 2004, PALAO has been upgraded (PALM-LGS) to support sodium laser guide star (LGS) operations using the macropulse/micropulse Chicago Sum-Frequency Laser (CSFL), built by University of Chicago (Section 3).

The PALAO optical bench is shown in Fig. 1. Key components include a 349-actuator Xinetics, Inc. electrostrictive deformable mirror (DM) sporting a 2 mm thick Zerodur facesheet. Of these, 241 actuators are actively controlled, yielding 16 subapertures across the telescope pupil diameter. The DM is located at an internal pupil, optically conjugated to the 5.1m primary mirror. The actuator grid is square on 7 mm pitch and is routinely operated with 4 microns of mirror surface stroke (using 0-100V drivers). The matched high-order Shack-Hartmann wavefront sensor (WFS), based on a SciMeasure Analytical Systems, Inc. "Little Joe" camera, contains a 80x80 pixel EEV39 CCD detector by EEV (now e2v Technologies). This sensor has been measured to achieve 3.7 e- rms read noise at ~500 frames per second (fps) and 6.4 e- rms read noise at 2000 fps. The wavefront reconstructor

computer performs detector flat-fielding, sky-subtraction, centroiding (in binned 2x2 pixel mode), and full vector-matrix-multiply reconstruction, then calculates PI servo control laws for the DM actuators and a separate fast steering mirror (FSM). Low-order wavefront sensing of natural guide stars (NGS) is accomplished using a 3x3 subaperture Shack-Hartmann WFS, based on a 2<sup>nd</sup> Little Joe camera having a hardware interface identical to the high-order WFS camera. A separate real-time reconstruction computer is used for the low-order sensing of tip/tilt and focus, with control signals folded into the FSM and DM signal path at the servo controller level. The system control architecture for PALAO is shown in Fig. 2. The high-order WFS resides on a linear translation stage to track the optical conjugation of the sodium layer, which varies by about 7 cm when slewing between 90 km and infinite object distance.

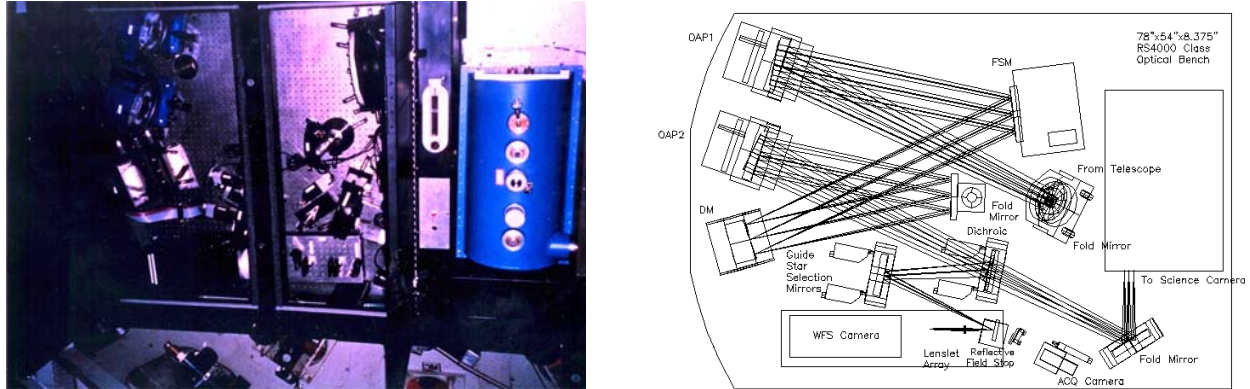


Fig. 1 (left) Photograph and (right) layout of the existing PALAO system, with enclosure doors opened. The blue dewar shown at right is the PHARO infrared camera/spectrograph/coronagraph (built by Cornell University). The PALAO instrument is approximately 76"x54"x30" in size.

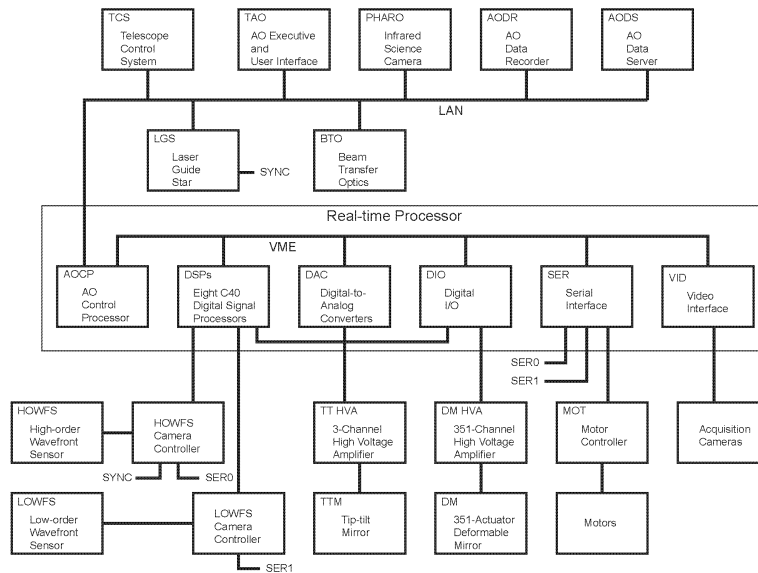


Fig. 2. Current architecture of the PALM-LGS system, highlighting the real-time wavefront reconstruction processor (proposed to be upgraded for PALM-3000).

PALAO has a comprehensive wavefront sensor telemetry data recording ability that greatly facilitates system optimization. Full high and low-order WFS camera pixel data (raw or flat-fielded) can be recorded at up to 400 Hz, while centroid data, subaperture flux, DM and FSM residual errors and commands, and system state are logged at up

to 2 kHz. A graphical user interface (GUI) provides real-time actuator position data displays and manages automated observing procedures, such as DM-to-lenslet registration, wavefront sensor background measurement, and on-the-fly loading of new reconstruction matrices. An expansive suite of IDL-based tools have been developed for more sophisticated engineering analysis of PALAO. No members of the Palomar AO development team are present during routine NGS science observing.

Fig. 3 depicts the recently implemented servo mirror system that transports the high-power sodium laser beam from the Coude lab of the Hale Telescope to a Laser Launch Telescope and beyond. A series of fast-acting quad-cell detectors ensure proper beam steering and are an integral part of the Laser Safety System. During propagation, the observatory dome floor is off-limits to personnel, with hardware interlocks on all access points. The wind screen is also deployed in the dome slit to eliminate the external view of the transferring beam.

First detection of sodium return light from the mesosphere was achieved on July 2, 2005, as shown in Fig. 4. This image was taken at best focus with the PALAO acquisition camera, currently a PULNIX 745-TE, which uses the entire aperture of the telescope (WFS subaperture images are expected to be very slightly smaller). During our initial tests, several non-optimized optics in the transfer system were used, as we awaited delivery of optimally coated optics. Total transmission of the Coude optics, transfer system, and laser launch telescope was measured in July 2005 to be 35% (from the laser frequency summing crystal to just beyond the launch telescope). Recently installed optics are expected to have increased transmission to >70%. Based on  $D_2$  return predicted by [1] and [2], we found the sodium concentration to be near its expected seasonal low, in the range  $1.8 - 2.4 \times 10^9$  atoms/cm<sup>2</sup>.

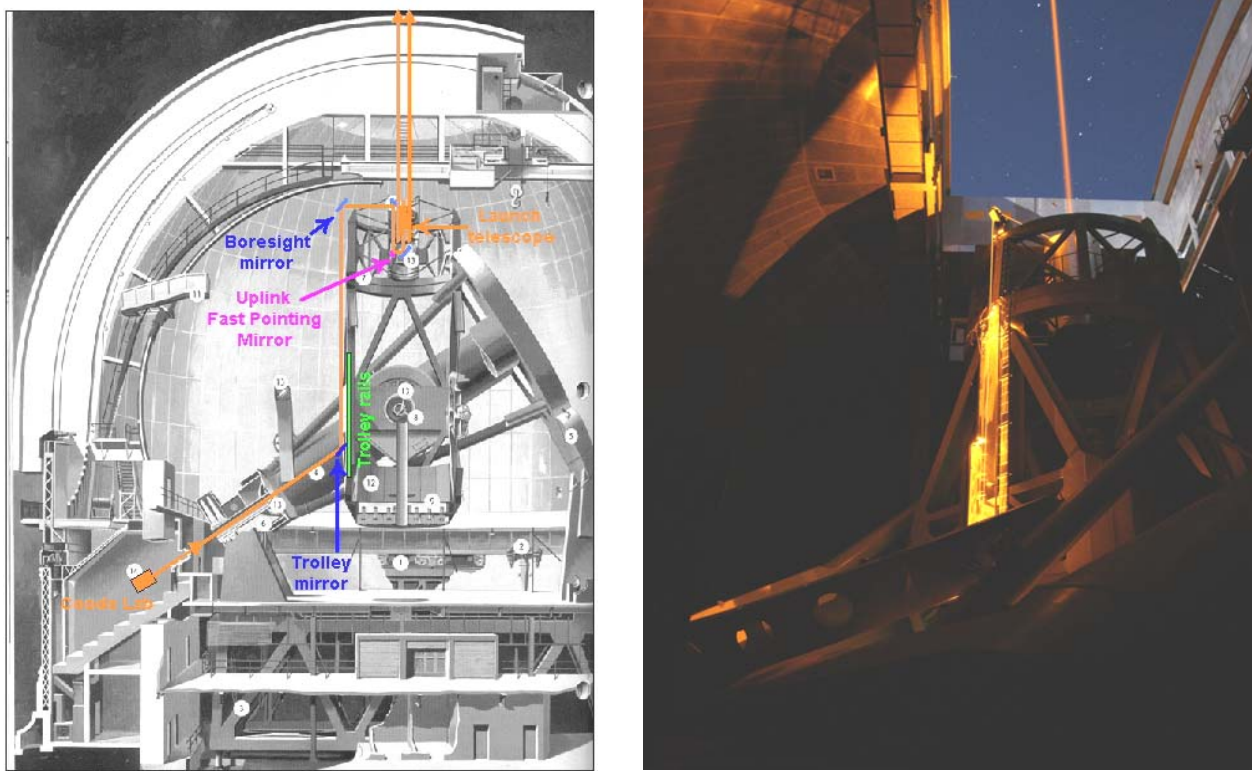


Fig. 3. Sodium laser beam propagation at Palomar Observatory. A series of servo controlled pointing and boresighting mirrors direct the beam to a custom 50 cm diameter launch telescope located on axis in the Hale Telescope prime focus housing.

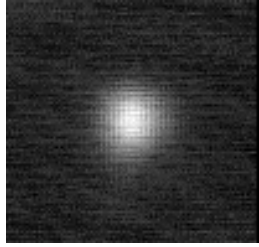


Fig. 4 Laser return from the Earth's mesospheric sodium layer on July 2, 2005, as seen in the full 5.1m aperture PALAO acquisition camera. Due to non-peak laser operation, non-optimized optical transmission and seasonally low sodium atom abundance, this return was measured to be equivalent to an  $m_v = 13.5$  natural guide star (as seen in our (unfiltered) CCD wavefront sensor). The FWHM of our beacon has to date been measured (full aperture) to be as small as 2.8 arcseconds (in 1.2 arcsecond seeing). Currently, engineering of the projection system and alignment of the laser launch telescope is underway in order to achieve the theoretical FWHM (approx. 1.8 arcseconds in 1.2 arcsecond seeing).

## 2. PALAO NATURAL GUIDE STAR PERFORMANCE

### Bright Natural Guide Star Performance

Using moderately bright natural guide stars PALAO has achieved wavefront errors as low as 170 nm rms, in 0.5 arcsec visible seeing and 190 nm rms, in 0.9 arcsec visible seeing. This corresponds to a scientific K-band imaging Strehl ratio of 80%, higher than reported for nearly all non-DoD adaptive optics systems. The outstanding image compensation of PALAO at infrared wavelengths, recovering at least 6 Airy rings of the diffraction pattern of the telescope, is shown in Fig. 5. Experimentally, we find that for bright stars the system is usually limited by wavefront fitting error (with our current projected actuator spacing of  $\sim 31$  cm) and occasionally by insufficient stroke. These limitations will be addressed PALM-3000 upgrade (Section 4). Occasionally, we also notice performance is limited by effects suspected to be associated with three non-functional actuators (all on the perimeter or outside the telescope pupil).

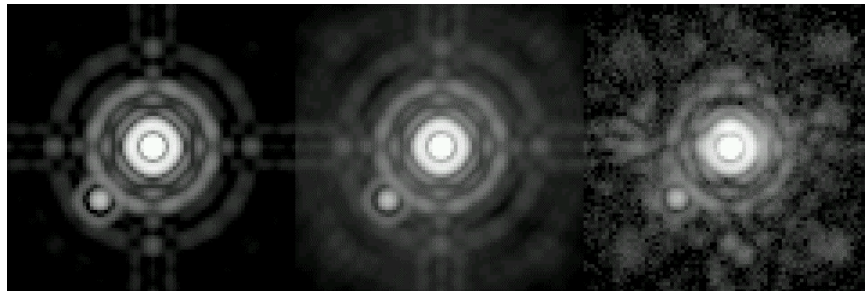


Fig. 5 PALAO comparison between (left) a theoretically perfect multispectral point spread function, (center) results from detailed closed-loop Monte Carlo simulations based on PALAO specifications, and (right) *actual* Palomar AO observations obtained September 2003 on an  $m_v = 7$  star in 0.9 arcsec visible seeing ( $r_0 = 11$  cm). The measured wavefront error is about 190nm rms (73% Strehl). ( $\lambda = 2.145 \mu\text{m}$ ,  $t_{\text{exp}} = 5$  seconds). The numerical simulations were performed using Caltech's ARROYO simulation library<sup>1</sup>, and includes the effects of a known 1% ghost reflection in the PHARO camera (lower left of image center).

<sup>1</sup> Caltech's extensive C++ adaptive optics modeling library, ARROYO, is available to the entire community under the GNU Public License (see <http://eraserhead.caltech.edu/>). ARROYO supports near-field and far-field diffractive wavefront propagation through arbitrary spectra turbulence, intricate pupil geometries, detailed Shack-Hartmann wavefront sensors, and definable DM influence functions. The ARROYO web site also provides an extensive set of instructional demonstrations useful when introducing AO concepts to students.

## Faint Natural Guide Star Performance

PALAO faint guide star performance is a strong function of seeing conditions and wind velocity profile. A snapshot of system performance from September 2004 is presented in Fig. 6. Full performance is achieved with natural guide stars (NGS) as faint as  $m_V \sim 11.5$ . Stable loop operation and partial (non-diffraction-limited) image compensation has been achieved on NGS as faint as  $m_V \sim 14.3$ .

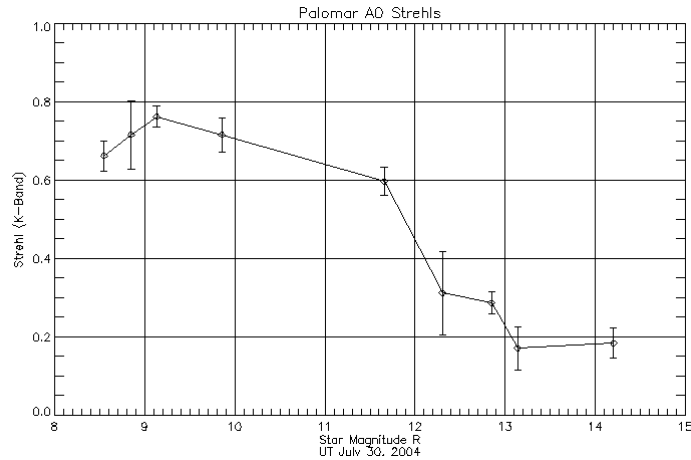


Fig. 6 Measured PALAO performance vs. NGS guide star magnitude. Interleaved seeing measurements ensured constant seeing conditions with median  $r_0$  value (at 0.5 microns) of 0.20 meters. Performance for sources brighter than about  $m_V = 10$  are capped by (then present) internal calibration errors between the AO system and science camera, which have since been improved (discussion below). We expect laser guide star return to have centroiding error equivalent to an  $m_V = 9$  star during favorable Fall sodium abundance conditions. During Spring, the return flux will be approximately 2 visual magnitudes fainter, but still usable at nearly full system performance.

## Modified Gerchberg-Saxton Wavefront Calibration

To help "raise the roof" of calibration-limited NGS performance shown in Fig. 6, members of our team (at JPL) have undertaken to reduce the calibration error between the AO system WFS and the infrared PHARO science camera (Section 5). To accomplish this, we used a Modified Gerchberg-Saxton (MGS) algorithm that exploits symmetrically defocused point spread functions, along with a pupil mask, to calculate the optical path difference of the wavefront at the exit pupil. Individual actuator gains ( $\mu\text{m}$  per Volt) must be measured to properly build an actuator sensitivity matrix. These can be determined by measuring a poked actuator's effect on the wavefront as seen in the MGS algorithm's reconstruction output. All 241 active actuators in the Palomar DM have been characterized by examining the MGS results from the (sparsely arrayed) poked wavefronts of nine separate patterns. Using this technique, minimum calibration errors have been reduced from about 100 nm rms to 44 nm rms. Future automation of this procedure is expected to allow approximately 30 nm rms calibration errors, which may also be optimized for each infrared / neutral density filter combination within PHARO.

## 3. CHICAGO SUM-FREQUENCY LASER

The Chicago Sum-Frequency Laser (CSFL) is a 7.5 W solid-state, mode-locked sodium laser based upon Nd:YAG sum-frequency generation of 1.06 micron and 1.32 micron transitions in the diode-pumped YAG crystal engines. The CSFL is a 2<sup>nd</sup> generation implementation of a design originated by Tom Jeys of MIT/LL [3], with diode-pumped YAG engines substantially re-engineered for improved thermal control. The laser pulse format consists of relative long 180 microsecond pulses emitted at up to 500 Hz repetition rate, thus having about 9% duty cycle. These so-called macropulses are themselves composed of a train of micropulses that result in a spectral bandwidth optimally matched to exploit the mesospheric  $D_2$  line without saturation. The CSFL is simple (alignable by two persons in one long day) and robust (shown to withstand transport from the 5.1m Telescope basement to the

Coude lab with no required internal realignment). A photograph of the CSFL in operation is shown in Fig. 7. Near-term upgrades include new high voltages drivers that will allow operation up to 800 Hz macropulse repetition rate (1,000 Hz goal).

As part of our upgrade strategy, we began testing of periodically poled stoichiometric lithium tantalate (PPSLT), within the CSFL in August 2005. We are investigating the sum-frequency conversion efficiency of these crystals in a non-mode-locked configuration. If sufficiently efficient, we expect to continue CSFL development toward 20 W power levels without mode locking, which will further simplify the laser system.

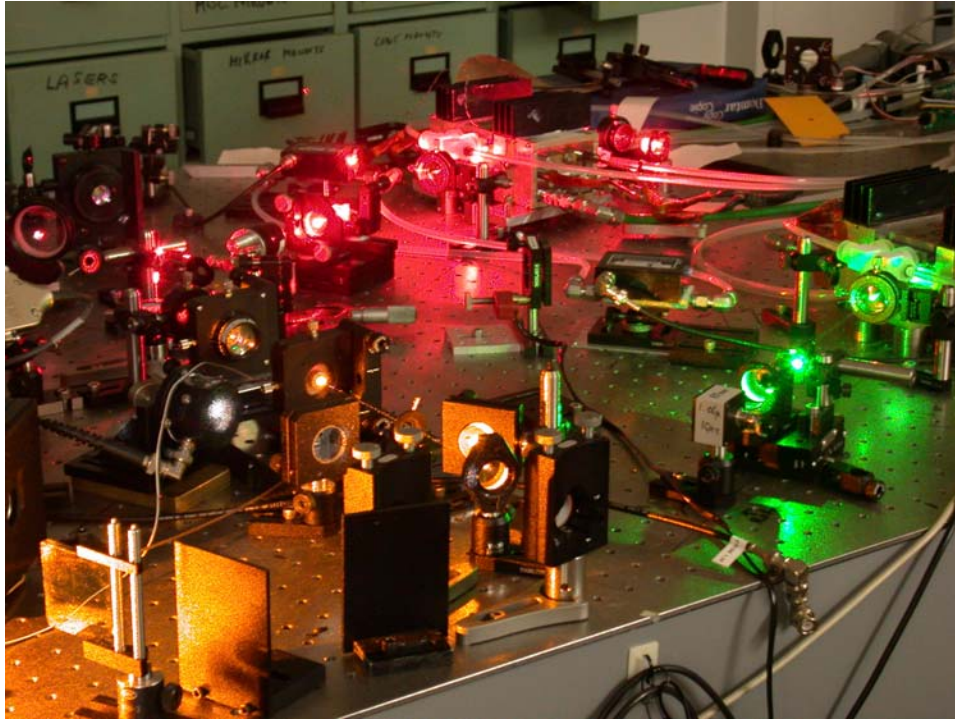


Fig. 7 The Chicago Sum-Frequency Laser (CSFL). Red and green light 2<sup>nd</sup> harmonics trace the infrared beams (top and right, respectively), which are frequency summed to produce 589.2 nm light (lower left). To date, 7.5 W of mode-locked macro/micropulse D<sub>2</sub> light has been generated with  $M^2 < 1.1$ .

#### 4. PLANNED PALM-3000 VISIBLE-LIGHT ADAPTIVE OPTICS UPGRADE

To further sharpen imaging resolution and to gain access to visible-light science bands, we are in the planning stages of a major upgrade to the PALAO system. The keynote of this upgrade will be the addition of a 4,356 (3,217 active) actuator Xinetics deformable mirror, to work in concert with the existing 349 actuator DM simultaneously providing greater spatial bandwidth of control and increased control stroke. Full implementation of the PALM-3000 upgrade also requires a new 128x128 pixel wavefront sensor camera and a major upgrade of the real-time wavefront processor computer. Coupled with Palomar's good astronomical site (5500' altitude), PALM-3000 promises to deliver the highest resolution astronomical AO images ever obtained.

Unlike previous generations of deformable mirror, the innovative Xinetics, Inc. Photonex Module technology features an entire actuator array formed into a monolithic ceramic block. Several of these blocks are then assembled into an array and bonded to a polished glass facesheet to form the final mirror. Prototypes of the PALM-3000 deformable mirror are illustrated in Fig. 8.

The upgraded PALM-3000 adaptive optics system will provide N=62 subaperture wavefront sensor sampling and N=63 deformable mirror actuator control across the diameter of the 5.1m telescope. This corresponds to 8.2 cm projected subaperture diameter, considerably finer than the 32 subapertures across the 3.6m class AEOS and SOR

telescopes (having ~11.2cm projected subaperture). Thus, PALM-3000 will have 86% greater actuator density than any current AO system, allowing unprecedented correction of atmospheric wavefronts and providing a unique astronomical testbed for exploring the next level of performance limiting phenomena. The Strehl ratios expected for this system are tabulated in Table 1 while an example error budget is presented in Table 2.

Table 1. Expected Strehl ratio performance of PALM-3000 on bright natural guide stars, under various seeing conditions (described by Fried's parameter,  $r_0$ ).

Seeing condition	$r_0(0.5\mu\text{m})$	RMS WFE	On-axis Strehl Ratio for $m_v=7$ star		
			0.4 micron	0.5 micron	0.7 micron
Superior	25 cm	80 nm	20%	36%	59%
Median	12 cm	99 nm	8%	19%	43%
Poor	5 cm	167 nm	--	--	11%

In superior seeing conditions, significant Strehl ratios will be obtained at even blue light (0.4  $\mu\text{m}$  wavelength), providing imaging resolution as fine as 78 nanoradians, the diffraction limit on the 5.1 meter telescope, twice the theoretical sharpness of Hubble Space Telescope. This unprecedented level of angular resolution will enable a variety of new observations on bright guide stars. Principal among these are geophysical studies of planetary surfaces (e.g. Io, Ganymede, Europa), mineralogical studies of asteroids (e.g. Vesta, Ceres, Pallas), direct surface imaging of sunspot activity on supergiant stars (e.g. Betelgeuse having diameter ~250 nanoradians),  $H_\alpha$  emissions from Mira variables, and (using the LGS system) astrometry of pre-main sequence binary stars, and studies of low-mass companions to nearby white dwarfs (there are 118 catalogued white dwarfs within 20 parsecs from Earth).

Table 2. Example error budget for PALM-3000 using a bright natural guide star ( $m_v = 7$ ) with  $r_0(0.5\mu\text{m}) = 12$  cm. This example yields a Strehl ratio of 43% at observing wavelength 0.7 $\mu\text{m}$ . PALM-3000 will also allow LGS operation in the red visible bands, at reduced Strehl, particularly during peak seasonal sodium column density.

Error source	Wavefront Error Contribution (nm)
Atmospheric fitting error ( $r_0(0.5\mu\text{m}) = 12$ cm)	24
Residual telescope fitting error (est. based on primary mirror test, 1995)	25
Residual AO system fitting error (est. based on AO calibration tests, 2005)	20
Residual instrument fitting error (est. made on instrument test, 1998)	20
Bandwidth error (1619 Hz sample rate, $f_0 = 43$ Hz, -3db rejection = 65 Hz)	56
Measurement error ( $m_v=7$ star, 2.5 e- read noise, 2x2 pixel sampling)	68
Anisoplanatism (for an on-axis target)	0
Tip/Tilt equivalent error ( $m_v = 7$ star)	11
Residual aliasing (after WFS input spatial filter)	3
Scintillation error in wavefront sensor (for Cerro Pachon 7-layer atmosphere, scintillation index = 0.15)	13
Residual differential atmospheric refraction (after atm. dispersion corrector)	5
<b>Total wavefront error (RMS)</b>	<b>99</b>

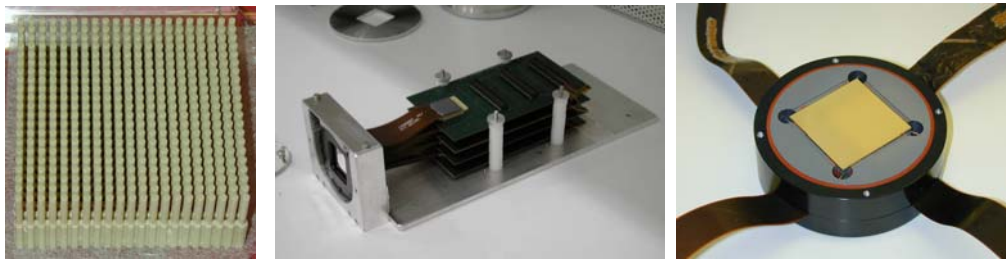


Fig. 8. The first example of a Xinetics 52.5 mm dimension actuator module shown (left) has 21 x 21 actuators on 2.5 mm pitch. The PALM-3000 mirror will consist of an array of 4 modules, each 33 x 33 actuator on ~1.7 mm pitch, bonded to a single continuous facesheet. A completed prototype Xinetics 32 x 32 actuator mirror (center and right) consisting of a single module with 1 mm pitch demonstrates the flex circuit solution for the many electrical interconnects needed for PALM-3000.

Fig. 9 shows the architecture we propose for the PALM-3000 real-time wavefront processor upgrade. The proposed hardware purchase (requested through the 2005 DoD DURIP solicitation) is for twelve quad DSP/dual FPGA boards plus a host computer, housed in a cPCI chassis. The AOCPC computer is retained, and continues to provide video and motor control functions as before. Its role as real-time host moves to the new real-time host processor, called RT0 in Fig. 9. Each of the twelve quad boards contains four 1 GHz TI C6416 DSPs and two Xilinx Virtex II XC2V3000 FPGAs. These are commercially available boards from Lyrtech, Inc. The DSPs each contain 4 16x16 bit hardware multipliers that are clocked at 1 GHz, and the FPGAs each contain 96 18x18 bit hardware multipliers that are clocked at 50 MHz.

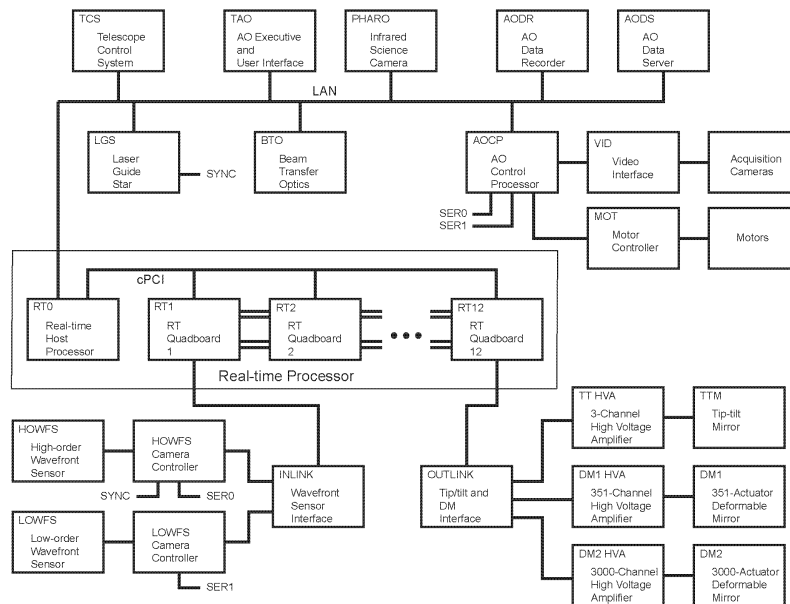


Fig. 9 Control architecture of the proposed PALM-3000 Adaptive Optics System.

## 5. PHARO SCIENCE CAMERA

The PALM-LGS system includes a capable and versatile back-end near-infrared instrument, PHARO (built by Cornell University, T. Hayward, PI). PHARO provides 25 and 40 milliarcsec plate scales on a 1024 x 1024

HgCdTe (HAWAII) array, as well as a medium resolution ( $R=1200$ ) grism spectroscopy mode and a versatile Lyot coronagraph capability. A variety of broad and narrow-band imaging filters are available covering the J, H, and K band atmospheric windows. The PALAO system allows the maximum 40 arcsec PHARO FoV to be offset some 45 arcsec from the optical axis of the telescope, allowing a total available field of regard of between 90 arcsec and 120 arcsec diameter. Experiments have been conducted with PALAO/PHARO using classical Lyot [4], [5] and four-quadrant phase mask nulling [6]. A subarray readout mode of PHARO allows 128x128 pixel regions to be read out at approximately 200 millisecond exposure times, allowing for research in AO-assisted speckle interferometry and speckle holography [7][8][9].

For visible imaging enabled by the proposed PALM-3000 upgrade, we shall convert a standard Palomar imaging camera, known as CCD13, for use in place of the PHARO camera. CCD13 contains a 1024x1024 Kodak CCD and is well understood by Palomar staff, allowing for an easy interface to the PALM-3000 system. CCD13 will allow narrow- and broad-band visible filter imaging and with modest reimaging optics allow for Nyquist sampling at the diffraction limit of blue light (about 8 milliarcseconds/pixel). In the longer term, we envision the addition of a visible spectrograph capability behind PALM-3000 (currently, we are in negotiations with a group based in the United Kingdom to bring their visible integral-field, resolution  $R=4000$  spectrograph to Palomar in 2008).

## 6. ACKNOWLEDGEMENTS

The authors would like to thank Ben Platt and Kent Wallace of JPL for optical engineering assistance, Dave Redding of JPL for assistance with the MGS calibration algorithm, and most importantly the dedicated staff of Palomar Observatory, particularly John Henning, Mike Doyle, Merle Sweet, Rick Burruss, Jeff Hickey, Jean Mueller, and Andrew Pickles. CSFL development has been supported by the National Science Foundation (NSF) and NSF's Center for Adaptive Optics (CfAO). The PALM-LGS installation at Palomar Observatory was made possible through the generous support of The Samuel Oschin Foundation.

## 7. REFERENCES

- 
- 1 d'Orgeville, C., Rigaut, F., and Ellerbroek, E., "LGS AO Photon Return Simulations and Laser Requirements for the Gemini LGS AO Program," Proc. SPIE 4007, 131-141 (2000).
  - 2 Kibblewhite, E. D., and Shi, F. "Design and field tests of an 8-W sum-frequency laser for adaptive optics", Proc. SPIE 3353, 300-319 (1998).
  - 3 Jeys, T. H., Brailove, A. A., and Mooradian, A., "Sum frequency generation of sodium resonance radiation," Appl. Optics, **28**, 2588-2591, (1989).
  - 4 Oppenheimer, B. R., Golimowski, D. A., Kulkarni, S. R., Matthews, K., Nakajima, T., Creech-Eakman, M., & Durrance, S. T. 2001, AJ, 121, 2189.
  - 5 Metchev, S. A. and Hillenbrand, L. A., "Initial Results from the Palomar Adaptive Optics Survey of Young Solar-Type Stars: A Brown Dwarf and Three Stellar Companions, ," AJ, 617:1330–1346, 2004.
  - 6 Haguenaer, P., Serabyn, E., Bloemhof, E. E., Troy, M., Wallace, J. K., "An off-axis four-quadrant phase mask (FQPM) coronagraph for Palomar: high-contrast near bright stars imager," Proc. SPIE 5905 (2005).
  - 7 Bates, R. H. T., Gough, P. T., and Napier, J. T., Astron. Astrophys., **22**, 319-320 (1973).
  - 8 Gonglewski, J.D., Voelz, D.G., Fender, J.S., Cayton, D.D., Spielbush, B.K., and Pierson, R.E., "First astronomical application of post detection turbulence compensation: Images of  $\alpha$ -Aurigae,  $\nu$ -Ursae Majoris and  $\alpha$ -Geminorum using self-referenced speckle holograph," Appl. Optics, **29**, 4527-4529 (1990).
  - 9 Dekany, R., *High-Angular-Resolution Astrometry and Array Phasing with Large Ground-Based Telescopes*, Ph.D. Dissertation, University of Arizona, (1994).